SJR (SCI-08)

INTERNATIONAL JOURNAL OF HYDROGEN ENERGY 36 (2011) 6553–6559

Available at www.sciencedirect.com

ScienceDirect

journal homepage: www.elsevier.com/locate/he

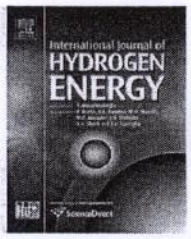

Synthesis of mesoporous-assembled TiO_2 nanocrystals by a modified urea-aided sol-gel process and their outstanding photocatalytic H_2 production activity

Singto Sakulkhaemaruethai [a], Thammanoon Sreethawong [b,c,*]

[a] Department of Chemistry, Faculty of Science and Technology, Rajamangala University of Technology, Klong 6, Thanyaburi, Pathumthani 12110, Thailand

[b] The Petroleum and Petrochemical College, Chulalongkorn University, Soi Chula 12, Phyathai Road, Pathumwan, Bangkok 10330, Thailand

[c] Center for Petroleum, Petrochemicals, and Advanced Materials, Chulalongkorn University, Bangkok 10330, Thailand

ARTICLE INFO

Article history:
Received 25 December 2010
Received in revised form
21 February 2011
Accepted 3 March 2011
Available online 31 March 2011

Keywords:
TiO_2
Urea
Sol-gel
Photocatalysis
Hydrogen production

ABSTRACT

Mesoporous-assembled TiO_2 nanocrystals with very high photocatalytic H_2 production activity were synthesized through a modified sol-gel process with the aid of urea as mesopore-directing agent, heat-treated under various calcination temperatures, and assessed for their photocatalytic H_2 production activity via water splitting reaction. The resulting mesoporous-assembled TiO_2 nanocrystals were systematically characterized by N_2 adsorption–desorption analysis, surface area and pore size distribution analyses, X-ray diffraction (XRD), scanning electron microscopy (SEM), and transmission electron microscopy (TEM). The experimental results showed that the photocatalytic H_2 production activity of the synthesized mesoporous-assembled TiO_2 nanocrystal calcined at 500 °C, which possessed very narrow pore size distribution, was extraordinarily higher than that of the commercially available P-25 TiO_2 and ST-01 TiO_2 powders.

1. Introduction

Nanostructured titanium dioxide (TiO_2), or titania, has been proven to be a promising functionalized material for a broad range of applications, particularly as the most effective photocatalyst for environmental purification [1–3] and for H_2 production via the photocatalytic water splitting process [4–9], because of its non-toxicity, inexpensiveness, and fascinating physicochemical properties. Up to now, nanocrystalline TiO_2 particles with a mesoporous structural network have been widely studied. Various processes, such as sol-gel [10], solvothermal [11], chemical vapor deposition [12], and precipitation [13], were developed for the synthesis of nanocrystalline TiO_2 particles as advanced materials. Among these processes, sol-gel is an efficient route for the synthesis of nanocrystalline mesoporous-structured TiO_2 that has been verified to be a promising photocatalyst for H_2 production via the photocatalytic water splitting reaction, as aforementioned. The combustion of H_2 can generate a huge amount of energy with water, or water vapor, as the only harmless by-product [14–16]. Since the generated H_2 does not involve CO_2 emission, it has been strongly believed to be a sustainable energy carrier in the near future for several applications, such as environmentally friendly automobiles

* *Corresponding author*. The Petroleum and Petrochemical College, Chulalongkorn University, Soi Chula 12, Phyathai Road, Pathumwan, Bangkok 10330, Thailand. Tel.: +66 2 218 4144; fax: +66 2 215 4459.
E-mail address: thammanoon.s@chula.ac.th (T. Sreethawong).

0360-3199/$ – see front matter
doi:10.1016/j.ijhydene.2011.03.005

and airplanes, domestic heating, and stationary power generation [17].

Urea is a major nitrogeneous end-product of human metabolism and product of petrochemical industry. It also plays a significant role in the marine nitrogen cycle, e.g. as sources both of excretion by many marine species [18] and of bacterial decomposition of nitrogeneous materials [19,20]. At present, the amount of produced urea tends to considerably increase because its production and consumption rates are being continuously increased, especially in petrochemical industry and in agricultural sector. It can be applied as agricultural fertilizer, cattle-feed supplement, and as a primary reactant for polymer synthesis [21]; however, currently there seems to have a surplus quantity of urea produced, and its further value-added use is thus inevitably required. Herein, the application of urea as a mesopore-directing agent in synthesizing nanocrystalline mesoporous-structured TiO_2 was the main focus. Although there have been several reports employing other conventional mesopore-directing agents, such as di-block copolymer (e.g. AT-18, AT-25, AT-50) [22], tri-block copolymer (e.g. P-123) [23], and ionic surfactant (e.g. CTAB) [24], for mesoporous-structured TiO_2 synthesis, the use of urea for such purpose offers some superior advantages to those agents, particularly the better economical viewpoint due to its less expensiveness and the requirement of less severe heat-treatment conditions when removing it from a mesoporous framework due to its smaller molecular structure.

In this work, the synthesis of mesoporous-assembled TiO_2 nanocrystals with highly enhanced photocatalytic H_2 production activity using a modified sol-gel process with the aid of urea was underlined. The purpose of this work was to investigate the influences of using urea as an efficient sol-inducing and mesopore-directing agent and calcination temperature on the characteristics of the synthesized mesoporous-assembled TiO_2 nanocrystals. The obtained mesoporous-assembled TiO_2 nanocrystals were subsequently applied for H_2 production via the photocatalytic water splitting reaction using methanol as a hole scavenger, as compared to commercially available TiO_2 powders.

2. Experimental

2.1. Materials

Tetraisopropyl orthotitanate (TIPT, $Ti(OCH(CH_3)_2)_4$) was supplied from Tokyo Chemical Industry Co., Ltd. Acetylacetone (ACA, $CH_3COCH_2COCH_3$) was supplied from Nacalai Tesque, Inc. Urea (NH_2CONH_2) was supplied from Wako Pure Chemical Industries, Ltd. All chemicals were analytical grade and used without further treatment. The TIPT was used as a titanium precursor. The ACA was used as a modifying agent to balance the hydrolysis and condensation rates of the titanium precursor. The urea was used as both sol-inducing agent and mesopore-directing agent. Commercially available TiO_2 powders, i.e. P-25 TiO_2 (supplied from Degussa, Nippon Aerosil Co., Ltd.) and ST-01 TiO_2 (supplied from Ishihara Co., Ltd.), were employed for comparative photocatalytic H_2 production activity testing.

2.2. Synthesis procedure

The mesoporous-assembled TiO_2 nanocrystals were synthesized via a modified sol-gel process with the aid of urea. In typical synthetic steps, a pre-determined amount of the ACA was first introduced into the TIPT with the TIPT-to-ACA molar ratio of 1:1. The mixture was then gently shaken until it was homogenized. Afterward, a 0.4 M urea aqueous solution was added to the ACA-modified TIPT mixture, where the TIPT-to-urea molar ratio was adjusted to a desired value of 4:1. The finally mixed solution was left on a magnetic stirrer and kept continuously stirring at 40 °C to accordingly obtain a transparent yellow sol solution. Then, the sol-gel transition was accomplished by placing the sol-containing solution into an oven kept at 80 °C for a week. Subsequently, the gel formed was dried overnight at 80 °C under atmospheric pressure to eliminate the solvent. The dried gel was calcined at various temperatures (i.e. 450, 500, and 550 °C) for 4 h to remove the urea molecules and to consequently produce the desired TiO_2 photocatalysts.

It should be noticed that the urea aqueous solution importantly behaves as a sol-inducing agent because the transparent yellow sol could not be obtained when using only pure water (without dissolved 0.4 M urea) as a hydrolyzing agent. In the absence of urea, the yellow precipitates formed immediately when blending the ACA-modified TIPT mixture with pure water, and such precipitates could no longer dissolve in the solution to obtain the sol even after stirring at 40 °C for several days.

2.3. Characterization techniques

The N_2 adsorption–desorption isotherms of the investigated photocatalysts were obtained by using a surface area analyzer (BEL Japan, BELSORP-18 Plus) operated at the liquid N_2 temperature of −196 °C. The Brunauer–Emmett–Teller (BET) approach was used to calculate specific surface area of the photocatalysts by using adsorption data over the relative pressure range of 0.05–0.35. The Barrett–Joyner–Halenda (BJH) approach was employed to determine pore size distribution and mean mesopore diameter by using desorption data of the isotherms. Each photocatalyst sample was degassed at 200 °C for 2 h to eliminate the moisture and volatile species adsorbed on its surface before the analysis. The crystalline phase present in the photocatalysts was investigated by using X-ray diffraction (XRD) technique. A rotating anode XRD system (Rigaku, PMG-A2) generating monochromated Cu Kα radiation with a continuous scanning mode at the rate of 2°/min was used to acquire XRD patterns under operating conditions of 35 kV and 15 mA. The photocatalyst morphology and particle size were investigated by using a scanning electron microscope (SEM, JEOL, JSM-6500FE) and a transmission electron microscope (TEM, JEOL, JEM-200CX) under operating voltages of 15 kV and 200 kV, respectively.

2.4. Photocatalytic H_2 production activity testing

Photocatalytic H_2 production via the water splitting reaction was carried out in a closed gas system. A controlled amount (0.2 g) of each individual photocatalyst was suspended in

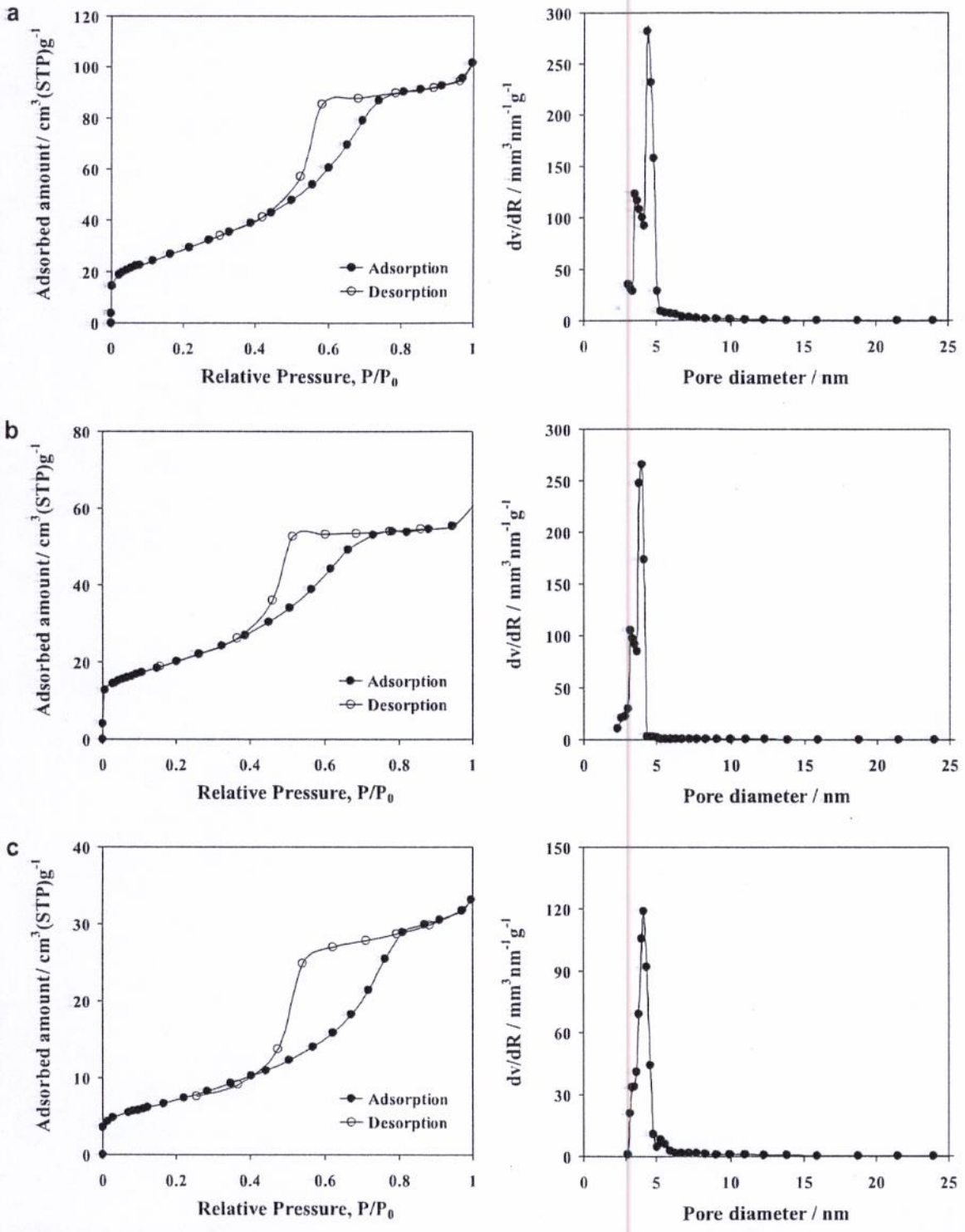

Fig. 1 – N_2 adsorption–desorption isotherms and pore size distributions of the synthesized mesoporous-assembled TiO_2 nanocrystal photocatalysts calcined at various temperatures: (a) 450 °C, (b) 500 °C, and (c) 550 °C.

a methanol aqueous solution (200 ml distilled water and 20 ml methanol) by magnetically stirring within an inner-irradiation Pyrex glass photoreactor. A 300 W high-pressure Hg lamp (WACOM Electric Co., Ltd.) was employed as the light source for UV irradiation. Before starting the photocatalytic reaction, the mixture was thoroughly purged by using Ar gas bubbling for 30 min in a dark environment. To avoid the temperature rise of the mixture during the photocatalytic reaction, cooling water was circulated through a Pyrex glass cylindrical jacket located around the light source to control the reaction

temperature at ~25–27 °C. The produced gaseous H_2 accumulated in the photoreactor headspace was intermittently collected and analyzed by an on-line gas chromatograph (Shimadzu, GC-8A Molecular sieve 5A, Ar gas) equipped with a thermal conductivity detector (TCD).

3. Results and discussion

3.1. Photocatalyst characterizations

The N_2 adsorption–desorption isotherms and pore size distributions of the synthesized TiO_2 nanocrystals calcined at various temperatures are shown in Fig. 1. All the samples clearly display the type IV-IUPAC adsorption–desorption isotherms with H2-type hysteresis loop. This observation implies the presence of well-developed mesoporous-assembled framework of the TiO_2 nanocrystals, which can be typically ascribed to the occurrence of capillary condensation of N_2 molecules inside the mesopores [25]. The pore size distributions of all the samples are also extremely narrow between 3 and 5 nm, indicating very uniform pore dimension of the synthesized mesoporous-assembled TiO_2 nanocrystals. Hence, the urea was proven to be a promising mesopore-directing agent for the synthesis of mesoporous-assembled TiO_2 nanocrystals. The textural properties, i.e. specific surface area, mean mesopore diameter, and total pore volume, of the synthesized mesoporous-assembled TiO_2 nanocrystals calcined at various temperatures and the commercially available TiO_2 powders are summarized in Table 1. It can be seen that the synthesized TiO_2 nanocrystals possessed the specific surface area in the range of 26.9–104.7 $m^2\ g^{-1}$, mean mesopore diameter in the range of 3.99–4.37 nm, and total pore volume in the range of 0.065–0.164 $cm^3\ g^{-1}$. The decreases in specific surface area and total pore volume with respect to the increase in calcination temperature may possibly result from the combined mesopore wall collapse and pore coalescence during the calcination step under a more severe temperature [26].

Fig. 2a shows the XRD patterns of the synthesized mesoporous-assembled TiO_2 nanocrystals calcined at various temperatures. The patterns exhibit the diffraction characteristic of the anatase TiO_2 phase due to the diffraction peaks at 2θ of about 25.2°, 37.9°, 47.8°, 53.8°, and 55.0°, corresponding to the (101), (004), (200), (105), and (211) crystalline planes (JCPDS Card No. 21-1272) [27], respectively. With increasing the calcination temperature, all the diffraction peaks became sharper and more intense, indicating the progress of crystallization of the TiO_2 nanocrystals. The crystallite sizes of the synthesized TiO_2 samples estimated from the Debye–Scherrer equation [28], using the XRD line broadening of (101) diffraction peak, are

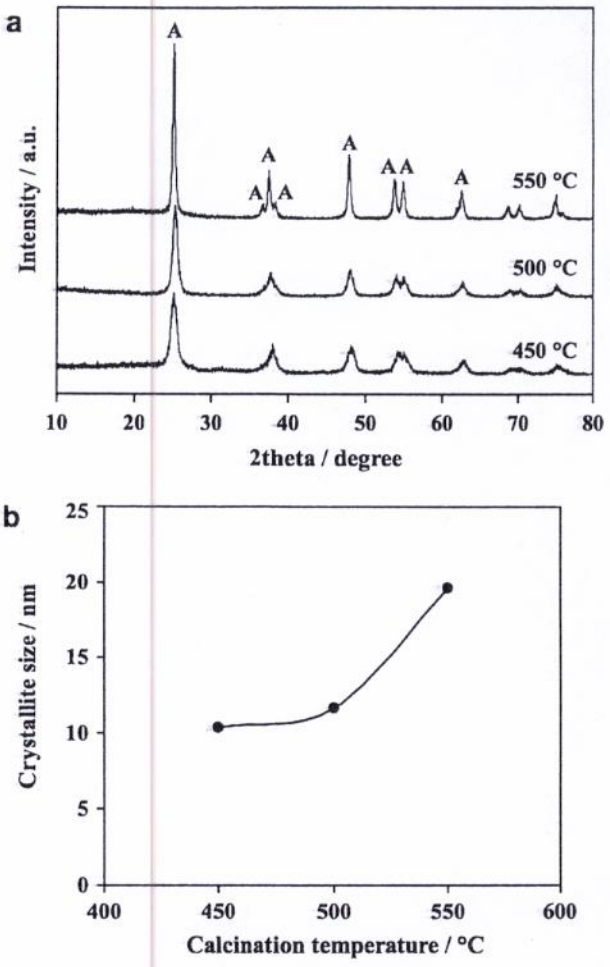

Fig. 2 – (a) XRD patterns and (b) crystallite sizes of the synthesized mesoporous-assembled TiO_2 nanocrystal photocatalysts calcined at various temperatures.

Table 1 – Physicochemical properties of the synthesized mesoporous-assembled TiO_2 nanocrystals calcined at various temperatures and the commercial TiO_2 powders.

Photocatalyst	Calcination temperature (°C)	Specific surface area ($m^2\ g^{-1}$)	Mean mesopore diameter (nm)	Total pore volume ($cm^3\ g^{-1}$)	Crystallite size[c] (nm)
Synthesized TiO_2	450	104.7	4.37	0.164	10.4 (A)
	500	71.9	3.99	0.110	11.6 (A)
	550	26.9	4.17	0.065	19.6 (A)
P-25 TiO_2	–	51.6[a]	–[a,b]	–[a,b]	20.7[a] (A), 29.9[a] (R)
ST-01 TiO_2	–	300[a]	–[a,b]	–[a,b]	10.4[a] (A)

a Sreethawong et al. [26].
b N_2 adsorption–desorption isotherms corresponds to IUPAC type II pattern.
c A = Anatase, R = Rutile.

reported in Table 1 and plotted as a function of calcination temperature in Fig. 2b. It was found that the TiO_2 crystallite sizes were approximately 10.4, 11.6, and 19.6 nm for the samples calcined at 450, 500, and 550 °C, respectively. The increase in the TiO_2 crystallite size clearly substantiates the growth of the TiO_2 nanocrystals upon the calcination at a higher temperature.

Fig. 3 illustrates the exemplified SEM and high resolution TEM images of the synthesized mesoporous-assembled TiO_2 nanocrystal calcined at 500 °C, which possessed a maximum photocatalytic H_2 production activity, as described later (Section 3.2). The SEM image clearly reveals the formation of TiO_2 clusters owing to the three-dimensional disordered assembly of several TiO_2 nanoparticles with quite uniform particle size (Fig. 3a). Each TiO_2 cluster size was in the range of approximately 20–50 nm. The assembly of a multitude of clusters is considered to be a reasonable cause of the existence of inter-cluster voids, which therefore resulted in the observed mesoporous-assembled structure of the synthesized TiO_2 nanocrystals. The particle size of the TiO_2 nanoparticles that assembled to form clusters was in the uniform and narrow range of approximately 10–15 nm, as can be clearly seen from the high resolution TEM image (Fig. 3b).

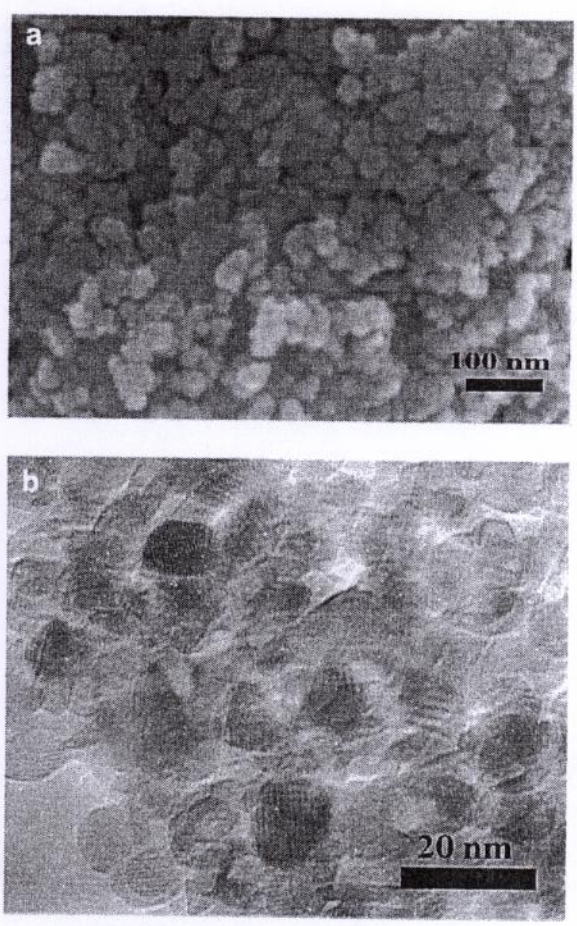

Fig. 3 – (a) SEM and (b) high resolution TEM images of the synthesized mesoporous-assembled TiO_2 nanocrystal photocatalyst calcined at 500 °C.

3.2. *Photocatalytic H_2 production activity*

The photocatalytic H_2 production activity of the synthesized mesoporous-assembled TiO_2 nanocrystals calcined at various temperatures was evaluated using the water splitting reaction with the methanol hole scavenger as compared to the commercially available P-25 TiO_2 and ST-01 TiO_2 powders, which possess non-mesoporous-assembled characteristic [29]. It should be initially reported from control experiments that there was no detectable H_2 gas produced in the absence of either UV light irradiation or suspended photocatalyst, so this points out that both of them are necessary for the water splitting reaction to photocatalytically produce H_2. Fig. 4 shows the H_2 production rate of the synthesized mesoporous-assembled TiO_2 nanocrystal photocatalysts as a function of calcination temperature. It can be clearly seen that the H_2 production rate remarkably increased from 332.7 to 409.2 μmol h^{-1} with increasing calcination temperature from 450 to 500 °C; nevertheless, it negatively decreased to 249.4 μmol h^{-1} with further increasing calcination temperature to 550 °C. These indicate a critical influence of the calcination temperature on the photocatalytic H_2 production activity. The observed results can be described by carefully taking the physicochemical properties of the synthesized TiO_2 nanocrystal photocatalysts into account. With initially increasing calcination temperature from 450 to 500 °C, the increase in H_2 production rate is plausibly because of the lower number of TiO_2 lattice defects due to the higher TiO_2 crystallinity observed from the XRD patterns (Fig. 2a), although the decrease in surface active sites due to the lower specific surface area of the synthesized TiO_2 nanocrystal photocatalyst was observed (Table 1). This suggests that the crystallinity of the synthesized TiO_2 nanocrystal photocatalyst exerts a more crucial effect on the photocatalytic H_2 production activity than the specific surface area in this calcination temperature range of 450–500 °C. In contrast, with further increasing calcination temperature from 500 to 550 °C, the decrease in H_2 production rate is plausibly because of the

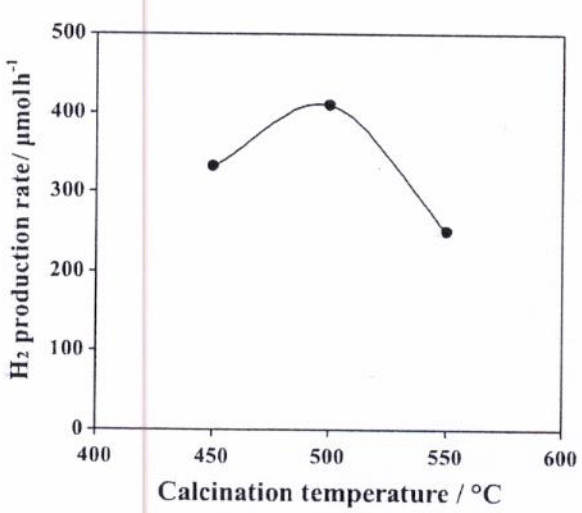

Fig. 4 – Photocatalytic H_2 production results of the synthesized mesoporous-assembled TiO_2 nanocrystal photocatalysts calcined at various temperatures.

lower surface active sites due to the large decrease in specific surface area, although the higher crystallinity was observed. This implies that the decrease in photocatalytic H_2 production activity in this calcination temperature range of 500–550 °C may be regulated by the specific surface area of the synthesized TiO_2 nanocrystal photocatalyst more than the crystallinity. It can then be concluded that the best synergy between the specific surface area (i.e. the surface active sites) and the crystallinity (i.e. the number of lattice defects) is required to attain the highest photocatalytic H_2 production activity of the mesoporous-assembled TiO_2 nanocrystal photocatalyst. Therefore, from the overall photocatalytic H_2 production activity results, the calcination temperature of 500 °C is proven as the most appropriate value for synthesizing the most effective mesoporous-assembled TiO_2 nanocrystal photocatalyst in this present work.

In addition, the photocatalytic H_2 production activity of the mesoporous-assembled TiO_2 nanocrystal photocatalyst was compared with that of the commercially available P-25 TiO_2 and ST-01 TiO_2 powders. The experimental results showed that the H_2 production rates of the P-25 TiO_2 and ST-01 TiO_2 powders were only 30.8 and 83.9 μmol h^{-1}, respectively, as compared to 409.2 μmol h^{-1} of the mesoporous-assembled TiO_2 nanocrystal photocatalyst calcined at 500 °C. These comparative results indicate that the H_2 production activity of such the synthesized mesoporous-assembled TiO_2 nanocrystal photocatalyst is approximately 13 and 5 folds higher than that of the P-25 TiO_2 and ST-01 TiO_2 powders, respectively. This clearly verifies the superior photocatalytic property of the synthesized TiO_2 nanocrystal photocatalyst to the commercially available TiO_2 powders. The low photocatalytic activity of the P-25 TiO_2 is possibly due to its 23% rutile TiO_2 content (with 77% anatase TiO_2 content), which leads to a lower driving force for water reduction as compared to the anatase TiO_2, due to its lower flat band potential level at very close to the H^+/H_2 potential level; whereas, the low photocatalytic activity of the ST-01 TiO_2 is possibly due to its large contents of bulk and surface defects originating from the imperfect crystallization [26], which leads to a much higher tendency for undesirable electron/hole recombination. Moreover, very less accessibility of reactant molecules (water molecules) to reach the surface active sites of these commercial TiO_2 powders for water reduction to cause the splitting for H_2 production stems from their non-mesoporous-assembled structure, as clearly shown in our previous works [26,30,31].

Hence, in overall, the mesoporous-assembled TiO_2 nanocrystal synthesized by the modified sol-gel process with the aid of urea and calcined at 500 °C is a very highly potential photocatalyst for H_2 production from the water splitting reaction since it provides extremely higher photocatalytic activity than the commercially available P-25 TiO_2 and ST-01 TiO_2 powders.

4. Conclusions

This work demonstrated that by applying urea as both sol-inducing agent and mesopore-directing agent for a modified sol-gel process, the mesoporous-assembled TiO_2 nanocrystals with high surface area, narrow pore size distribution, small crystallite size, and high potential to be used as the efficient photocatalyst for H_2 production from water splitting reaction were successfully synthesized. It was found that the synthesized mesoporous-assembled TiO_2 nanocrystal photocatalyst calcined at 500 °C exhibited very considerably high photocatalytic H_2 production activity, especially much greater than the commercially available P-25 TiO_2 and ST-01 TiO_2 powders.

Acknowledgments

This work was financially supported by the Research Grant for Mid-Career University Faculty (RMU) co-funded by the Thailand Research Fund (TRF); the Commission on Higher Education, Thailand; and Chulalongkorn University, Thailand. The authors would also like to thank the Sustainable Petroleum and Petrochemicals Research Unit, Center for Petroleum, Petrochemicals, and Advanced Materials, Chulalongkorn University, Thailand.

REFERENCES

[1] Tachikawa T, Fujitsuka M, Majima T. Mechanistic insight into the TiO_2 photocatalytic reactions: design of new photocatalysts. J Phys Chem C 2007;111:5259–75.
[2] Hoffmann MR, Martin ST, Choi W, Bahnemann DW. Environmental applications of semiconductor photocatalysis. Chem Rev 1995;95:69–96.
[3] Carp O, Huisman CL, Reller A. Photoinduced reactivity of titanium dioxide. Progr Solid State Chem 2004;32:33–177.
[4] Ni M, Leung MKH, Leung DYC, Sumathy K. A review and recent developments in photocatalytic water-splitting using TiO_2 for hydrogen production. Renew Sustain Energy Rev 2007;11:401–25.
[5] Matsuoka M, Kitano M, Takeuchi M, Tsujimaru K, Anpo M, Thomas JM. Photocatalysis for new energy production: recent advanced in photocatalytic water splitting reactions for hydrogen production. Catal Today 2007;122:51–60.
[6] Sreethawong T, Suzuki Y, Yoshikawa S. Photocatalytic evolution of hydrogen over mesoporous TiO_2 supported NiO photocatalyst prepared by single-step sol-gel process with surfactant template. Int J Hydrogen Energy 2005;30:1053–62.
[7] Sreethawong T, Yoshikawa S. Enhanced photocatalytic hydrogen evolution over Pt supported on mesoporous TiO_2 prepared by single-step sol-gel process with surfactant template. Int J Hydrogen Energy 2006;31:786–96.
[8] Dholam R, Patel N, Adami M, Miotello A. Physically and chemically synthesized TiO_2 composite thin films for hydrogen production by photocatalytic water splitting. Int J Hydrogen Energy 2008;33:6896–903.
[9] Huang CW, Liao CH, Wu JCS, Liu YC, Chang CL, Wu CH, et al. Hydrogen generation from photocatalytic water splitting over TiO_2 thin film prepared by electron beam-induced deposition. Int J Hydrogen Energy 2010;35:12005–10.
[10] Su C, Hong BY, Tseng CM. Sol-gel preparation and photocatalysis of titanium dioxide. Catal Today 2004;96:119–26.
[11] Kominami H, Kohno M, Takada Y, Inoue M, Inui T, Kera Y. Hydrolysis of titanium alkoxide in organic solvent at high temperatures: a new synthetic method for nanosized, thermally stable titanium (IV) oxide. Ind Eng Chem Res 1999;38:3925–31.

[12] Nakaso K, Okuyama K, Shimada M, Pratsinis SE. Effect of reaction temperature on CVD-made TiO_2 primary particle parameter. Chem Eng Sci 2003;58:3327–35.
[13] Nam HD, Lee BH, Kim SJ, Jung CH, Lee JH, Park S. Preparation of ultrafine crystalline TiO_2 powders from aqueous $TiCl_4$ solution by precipitation. Jpn J Appl Phys 1998;37:4603–8.
[14] Wallace JS, Ward CA. Hydrogen as a fuel. Int J Hydrogen Energy 1983;8:255–68.
[15] White CM, Steeper RR, Lutz AE. The hydrogen-fueled internal combustion engine: a technical review. Int J Hydrogen Energy 2006;31:1292–305.
[16] Midilli A, Dincer I. Hydrogen as a renewable and sustainable solution in reducing global fossil fuel consumption. Int J Hydrogen Energy 2008;33:4209–22.
[17] Balat M. Potential importance of hydrogen gas as a future solution to environmental and transportation problems. Int J Hydrogen Energy 2008;33:4013–29.
[18] Antia NJ, Harrison PJ, Oliveira L. The role of dissolved organic nitrogen in phytoplankton nutrition, cell biology and ecology. Phycologia 1991;30:1–89.
[19] Price NM, Harrison PJ. Comparison of methods for the analysis of dissolved urea in seawater. Mar Biol 1987;94:307–19.
[20] Goeyens L, Kindermans N, Yusuf MA, Elskens M. A room temperature procedure for the manual determination of urea in seawater. Estuar Coast Shelf Sci 1998;47:415–8.
[21] Vaio N, Cabrera ML, Kissel DE, Rema JA, Newsome JF, Calvert VH. Ammonia volatilization from urea-based fertilizers applied to tall fescue pastures in Georgia, USA. Soil Sci Soc Am J 2008;72:1665–71.
[22] Kim DS, Han SJ, Kwak SY. Synthesis and photocatalytic activity of mesoporous TiO_2 with the surface area, crystallite size, and pore size. J Colloid Interface Sci 2007; 316:85–91.
[23] Kim DS, Kwak SY. The hydrothermal synthesis of mesoporous TiO_2 with high crystallinity, thermal stability, large surface area, and enhanced photocatalytic activity. Appl Catal A Gen 2007;323:110–8.
[24] Narayanaswamy A, McBride J, Swafford LA, Dhar S, Budai JD, Feldman LC, et al. Synthesis and characterization of porous TiO_2 with wormhole-like framework structure. J Porous Mater 2008;15:21–7.
[25] Rouquerol F, Rouquerol J, Sing K. Adsorption by powders and porous solid: principle, methodology, and applications. San Diego: Academic Press; 1999.
[26] Sreethawong T, Suzuki Y, Yoshikawa S. Synthesis, characterization, and photocatalytic activity for hydrogen evolution of nanocrystalline mesoporous titania prepared by surfactant-assisted templating sol-gel process. J Solid State Chem 2005;178:329–38.
[27] Smith JV. X-ray powder data file. American Society for Testing Materials; 1960.
[28] Cullity BD. Elements of X-ray diffraction. Reading, MA: Addison-Weslay Pub. Co; 1978.
[29] Jantawasu P, Sreethawong T, Chavadej S. Photocatalytic activity of nanocrystalline mesoporous-assembled TiO_2 photocatalyst for degradation of methyl orange monoazo dye in aqueous wastewater. Chem Eng J 2009;155:223–33.
[30] Sreethawong T, Laehsalee S, Chavadej S. Comparative investigation of mesoporous- and non-mesoporous-assembled TiO_2 nanocrystals for photocatalytic H_2 production over N-doped TiO_2 under visible light irradiation. Int J Hydrogen Energy 2008;33:5947–57.
[31] Sreethawong T, Junbua C, Chavadej S. Photocatalytic H_2 production from water splitting under visible light irradiation using Eosin Y-sensitized mesoporous-assembled Pt/TiO_2 nanocrystal photocatalyst. J Power Sources 2009;190:513–24.

SJR SCImago Journal & Country Rank

EST MODUS IN REBUS
Horatio (Satire 1,1,106)

Home
Journal Rankings
Journal Search
Country Rankings
Country Search
Compare
Map Generator
Help
About Us

Journal Search

Search query

in Journal Title Search

Exact phrase

International Journal of Hydrogen Energy

Country: Netherlands

Subject Area: Chemistry

Subject Category: Electrochemistry

Publisher: Elsevier BV. **Publication type:** Journals. **ISSN:** 03603199

Coverage: 1976-2011

H Index: 89

Scope:

The International Journal of Hydrogen Energy provides scientists and engineers throughout the world with a central vehicle for the exchange [...]
Show full scope

Charts Data

Show this information in your own website

Display journal title

Just copy the code below and paste within your html page:
<a href="http://www.scimagojr

How to cite this website?

SJR is developed by:

SCIMAGO LAB

Powered by SCOPUS

SJR indicator vs. Cites per Doc (2y)

The SJR indicator measures the scientific influence of the average article in a journal, it expresses how central to the global scientific discussion an average article of the journal is. Cites per Doc. (2y) measures the scientific impact of an average article published in the journal, it is computed using the same formula that journal impact factor ™ (Thomson Reuters).

Citation vs. Self-Citation